JOURNAL OF MATERIALS SCIENCE 33 (1998) 3313–3319

Study of polyethylene pipe resins by a fatigue test that simulates crack propagation in a real pipe

A. SHAH, E. V. STEPANOV, M. KLEIN*, A. HILTNER‡, E. BAER
Department of Macromolecular Science, Case Western Reserve University, Cleveland, OH 44106, USA

A fatigue test that simulates the step-wise crack propagation found in pipes in the field, and uses a standard compact-tension specimen, was employed to study and rank crack resistance of various pipe resins. The thermal history during compression moulding of the test specimens strongly affected fracture kinetics. It was found that crack-resistant properties of in-service pipe were best reproduced if compression-moulded plaques were fast cooled under load. This procedure was used to prepare specimens from candidate pipe resins for fatigue testing. The resins were compared in terms of discontinuous crack growth kinetics. The ranking based on resistance to fatigue crack propagation correlated with results of a standard PENT creep test. However, fatigue failure times were an order of magnitude less than the standard creep times. After comparing the initiation and failure times of the resins with detailed kinetics of step-wise crack propagation, a simplified and rapid procedure is proposed which calls for evaluating only the first jump after initiation. © *1998 Kluwer Academic Publishers*

1. Introduction

A considerable need for predicting reliability of polyethylene pipes for natural gas distribution has motivated development of failure tests specifically intended for pipe materials [1–5]. Because pipes need to maintain their integrity over decades, testing under laboratory conditions requires significant fracture acceleration while conserving the crack growth mechanism inherent for field failure. Extensive experiments show that the main features of the field failure, such as periodical arrest and step-wise character of crack propagation [6, 7], can be reproduced in the laboratory using creep at elevated temperatures [8]. Good correlation between the frequency of pipe damage in the field and the ranking by the (PENT) creep test designed especially for polyethylene pipe resins (ASTM F 1473-94) was displayed [9]. However, for a new generation of pipe resins, testing materials by creep can require many months, even at elevated temperatures [5, 10]. Tests employing a fatigue crack propagation mechanism also reproduce the salient features of the field failure [11, 12]. In comparison to creep, fatigue can accelerate fracture by up to three orders of magnitude; resulting failure times become a matter of days or hours rather than months. A fatigue test conducted at room temperature also has the advantage of avoiding the possible effects of annealing, especially for branched polyethylenes which are usually characterized by a broad premelting temperature region [13]. Annealing can change the character of the fracture, making it different from lower temperature field failure. These advantages make fatigue more attractive than creep for evaluating pipe materials and possibly for predicting their lifetime [14–16].

Crack resistance of pipe resins depends on material morphology and process history [13, 17]. Furthermore, crack propagation in a real pipe proceeds under complex loading conditions determined by the pipe geometry. Testing specimens cut from a real pipe and conserving the pipe curvature would lead to the most objective results. Earlier investigations of the step-wise mechanism of crack propagation in real pipe followed this approach [2, 12, 18]. However, it becomes impractical to evaluate all new candidate resins for pipe applications by first moulding them into pipe. Moreover, the use of specimens of non-standard geometry which experience perceptible deformation upon loading presents difficulties in analysing the test data and comparing results for pipes of different dimensions. For these reasons, a method for fatigue testing a standard compact-tension specimen that reproduces and simulates step-wise crack propagation in a real pipe has been developed and experimentally verified [19]. Having correlated local stress distribution in specimens of compact-tension and real-pipe arc-shaped geometries (cut from the same pipe material), the dimensions, notch and fatigue loading parameters for the testing protocol have been defined. It is now

*900G 24th Street N.W., Washington, DC 20037, USA.
‡Author to whom all correspondence should be addressed.

0022–2461

possible to test and rank polyethylene pipe resins using a standard compact-tension specimen prepared by compression moulding. It is essential, however, that the fatigue crack resistance of the compression-moulded material be the same as in a real pipe.

In the present work, we investigate the effect of cooling conditions on the fatigue failure of compression mouldings in order to define a thermal history that produces laboratory specimens displaying the same fatigue crack resistance as extruded pipe. Furthermore, we perform a trial ranking of five polyethylene resins to develop a fatigue testing protocol that simulates step-wise crack propagation in a real pipe.

2. Experimental procedure

2.1. Materials

The material referred to as real pipe resin was made from 16 in. (~40.6 cm) outer diameter (medium density polyethylene (MDPE) gas pipe extruded from category II PE-2406 U DuPont Aldyl A resin [19]. The pipe was cut into small pieces 3–5 mm in size with a band saw for subsequent compression moulding. Four candidate pipe resins (identified as A, B, C and D) were obtained from the Gas Research Institute, Chicago, IL, in the form of pellets. Data on the performance of these resins in the standard PENT creep test (ASTM F 1473-94) were supplied by Uponor Aldyl Company.

Densities of materials were determined at room temperature using a density gradient column prepared from solutions of isopropanol and water in accordance with ASTM D 1505-85. Weight fraction of crystallinity, ω_c, was calculated from the density, ρ, by the relationship

$$\omega_c = \frac{\rho_c(\rho_a - \rho)}{\rho(\rho_a - \rho_c)} \quad (1)$$

where $\rho_c = 1000\ \mathrm{kg\,m^{-3}}$ and $\rho_a = 855\ \mathrm{kg\,m^{-3}}$ are the densities of the crystalline and amorphous components of polyethylene, respectively [20]. Reported densities were the average of five samples from each of three locations: both sides and the middle of a compression moulded plaque.

2.2. Compression moulding

Pellets were pressed at 190 °C with a preheat time of 20 min at zero load and 15 min under pressure of 20 MPa. Then the pressure was quickly raised and lowered ten times between the pressure limits of 20 and 40 MPa. The pressure was cycled to remove air bubbles which could have led to voids in the plaque. As a final step, the plaque was kept under constant pressure of 40 MPa for 5 min. The thickness of the plaque was 17 mm. Plaques were prepared with three cooling conditions: cooled in the press overnight at a rate of $0.5\ ^\circ\mathrm{C\,min^{-1}}$ (slow-cooled), cooled at a rate of $30\ ^\circ\mathrm{C\,min^{-1}}$ achieved by circulating cold tap water through the press (fast-cooled), and quenched in ice–water (quenched).

The $30\ ^\circ\mathrm{C\,min^{-1}}$ rate provided a cooling rate similar to that of a specimen quenched in ice–water yet under pressure. In this case, the cooling time of about 6 min correlated with a characteristic time $\tau \cong l^2/\pi^2\chi \cong 5$ min of natural cooling of $l = 17$ mm thickness plaque. The latter was estimated with thermal diffusivity $\chi \cong 10^{-7}\ \mathrm{m^2\,s^{-1}}$ [21] in accordance with heat transfer calculations for flat geometry [22].

2.3. Specimens

The dimensions of the compact-tension specimen were defined previously [19]: the thickness of the specimen $B = 13$ mm, the length defined as the distance between the line connecting the centres of the pin holes and the unnotched outer edge of the specimen $W = 26$ mm, the height to length ratio 1.2, and notch length $a = 12.5$ mm. All dimensions met the requirements of ASTM D 5045-93. With these dimensions, and in the range of fatigue loads specified below, fracture of a compact-tension specimen proceeded by the same mechanism and with the same rate as in real pipe loaded with the same stress intensity factor at the notch tip [19].

A control specimen of real pipe was cut from the pipe wall as described previously [19]. Specimens of candidate pipe resins were machined from compression-moulded plaques.

The specimens were notched in two steps. The initial part of the notch (10 mm) was made by saw, and the final one (2.5 mm) by a razor blade. The razor blade was mounted on a device which drove it into the specimen at a controlled speed of $1\ \mu\mathrm{m\,s^{-1}}$. A fresh razor blade was used to notch each specimen.

2.4. Fatigue testing

Mechanical fatigue units capable of applying very stable and accurate (± 0.5 N) sinusoidal loads were used to conduct the fatigue tests. The minimum to maximum load ratio, R, in a fatigue loading cycle was maintained at 0.1 for an all-tension cycle. Maximum load was varied in the range of 250–300 N, which produced a maximum stress intensity factor at the notch tip $K_{I,\max} = 1.0$–$1.3\ \mathrm{MPa\ m^{1/2}}$. The test frequency was 1 cycle $\mathrm{s^{-1}}$ in order to render hysteretic heating of the test specimen negligible.

The load and crosshead displacement were recorded by computer every 1000 cycles during the entire experiment. A manual zoom macrolens attached to a monochrome video camera was used to observe the craze front (an intensely deformed plastic zone which develops at the crack root [8, 12]) and to measure the crack depth during crack propagation. The output of the camera was routed through a VCR to a video monitor and, when the experiment was unattended, a videocassette recorded the experiment for later playback.

After each experiment, fractographic analysis was performed. Fracture surfaces were first examined under the light-microscope, and the photomicrographs presented are bright-field images using normal incidence illumination. Specimens were subsequently

coated with 9 nm gold for scanning electron microscope (SEM) observation in a Jeol JXA 50A instrument.

Every test was performed twice with specimens prepared from different compression moulded plaques to ascertain reproducibility of results.

3. Results and discussion

3.1. Effect of cooling conditions

Fatigue results for specimens prepared from compression-moulded plaques and control specimens cut from pipe are compared in Table I. Tests were performed with the notch tip stress intensity factor in the range of $K_{I,\max} = 1.0$–1.3 MPa m$^{1/2}$ which best reproduced the mechanism of step-wise crack growth in real pipe [19]. If $K_{I,\max}$ was lower, brittle crack growth lost the discontinuous character; if $K_{I,\max}$ was higher, fast ductile fracture resulted.

Fracture surfaces for tests with $K_{I,\max} = 1.2$ MPa m$^{1/2}$ are shown in Fig. 1. Crack propagation in all specimens was discontinuous. The well-resolved striations on the fracture surface indicated the crack arrest lines, the first one coinciding with the notch tip. During arrest, the crack remained stationary for several tens of thousands of cycles. A crack jump ahead to the next arrest position required a comparatively short time of only thousands of cycles. The crack arrest time was associated with the lifetime of the damage zone ahead the crack tip. Fracture surfaces indicated that the damage zone had a highly non-uniform structure. Dense arrest lines were the traces of the broken membrane that had formed at the arrested crack root. Broken fibrils in the regions between arrest lines were remnants of a cavitated zone in front of the membrane.

A crack jump began with the appearance of holes in the membrane, which quickly increased in size and coalesced until the membrane ruptured. Because the next membrane was immediately visible through the holes, the cavitated zone ahead of the membrane must have broken before the membrane itself began to rupture. Membrane rupture resulted in incremental crack growth and a sharp increase of the crosshead displacement. Crack initiation was taken as the first jump. The duration between jumps was defined as the time between the beginning of consecutive membrane ruptures, and was obtained from the video record. The jump length was taken as the distance between corresponding arrest lines on the fracture surface.

Detailed data on the first three jumps of step-wise fatigue crack propagation in the compression moulded materials are presented in Table II. The conditions used to cool the compression-moulded samples affected resistance to fatigue crack propagation dramatically. The parameter which was most

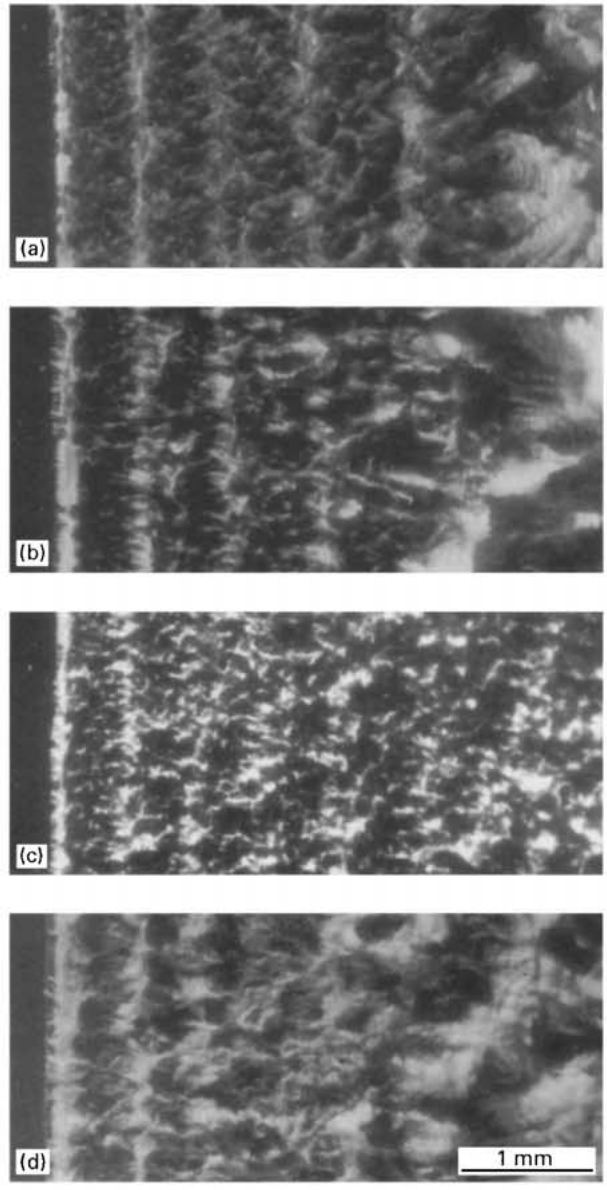

Figure 1 Fracture surfaces of compact tension specimens tested at an initial stress intensity factor of 1.2 MPa m$^{1/2}$: cut from (a) pipe, and compression-moulded (b) fast-cooled, (c) slow-cooled, and (d) quenched plaques.

TABLE I Effect of cooling conditions on fatigue crack initiation and failure

Material	Density (g/cm^3)	Crystallinity (Density)	$K_{I,\max} = 1.3$ MPa m$^{1/2}$		$K_{I,\max} = 1.2$ MPa m$^{1/2}$		$K_{I,\max} = 1.0$ MPa m$^{1/2}$	
			Cycles to initiation* (thousand)	Cycles to failure (thousand)	Cycles to initiation* (thousand)	Cycles to failure (thousand)	Cycles to initiation* (thousand)	Cycles to failure (thousand)
cut from pipe	0.9385 ± 0.0005	61%	74 ± 6	211 ± 14	65 ± 6	280 ± 30	80 ± 5	580 ± 20
Fast cooled	0.9397 ± 0.0003	62%	65 ± 5	234 ± 20	65 ± 6	275 ± 35	82 ± 6	560 ± 30
Slow cooled	0.9430 ± 0.0003	64%	35 ± 3	130 ± 7	35 ± 3	160 ± 10	—	—
Quenched	0.9380 ± 0.0005	61%	—	—	80 ± 10	415 ± 25	—	—

*duration to 1st jump

TABLE II Effect of cooling conditions on crack jump parameters

$K_{I,max}$ MPa $(m)^{\frac{1}{2}}$	Material	Length of jump 1 (mm)	Duration between jump 1 and 2 (thousand)	Length of jump 2 (mm)	Duration between jump 2 and 3 (thousand)	Length of jump 3 (mm)	Duration between jump 3 and 4 (thousand)
1.3	Cut from pipe	0.85 ± 0.05	40 ± 8	0.85 ± 0.05	34 ± 8	0.90 ± 0.05	35 ± 8
	Fast cooled	0.80 ± 0.08	45 ± 6	0.80 ± 0.08	34 ± 10	0.85 ± 0.08	30 ± 10
	Slow cooled	0.70 ± 0.04	20 ± 3	0.70 ± 0.06	20 ± 3	0.70 ± 0.08	15 ± 3
1.2	Cut from pipe	0.65 ± 0.05	58 ± 7	0.70 ± 0.05	46 ± 7	0.75 ± 0.05	44 ± 10
	Fast cooled	0.65 ± 0.05	50 ± 6	0.66 ± 0.04	47 ± 7	0.70 ± 0.08	35 ± 7
	Slow cooled	0.65 ± 0.04	30 ± 3	0.64 ± 0.06	20 ± 3	0.64 ± 0.08	20 ± 3
	Quenched	0.70 ± 0.10	70 ± 7	0.60 ± 0.15	65 ± 10	0.60 ± 0.20	65 ± 10
1.0	Cut from pipe	0.43 ± 0.04	65 ± 5	0.43 ± 0.04	65 ± 15	0.43 ± 0.04	65 ± 15
	Fast cooled	0.42 ± 0.06	68 ± 5	0.44 ± 0.06	50 ± 10	0.48 ± 0.06	50 ± 10

strongly influenced by thermal history was the duration between jumps. Because the impact of the cooling conditions on the jump length was not appreciable, differences in the durations directly resulted in different crack propagation rates and, hence, different failure times (Table I).

The effect of thermal history was first examined with $K_{I,max} = 1.2\ MPa\,m^{1/2}$ and then verified with two other values of maximum stress intensity factor. Specimens prepared from plaques quenched in ice–water showed very different fatigue behaviour from that of control specimens cut from pipe, as indicated by significantly higher initiation and failure times (Table I). On the fracture surfaces, the well-resolved striations of the control specimen (Fig. 1a) contrasted with thick and non-uniform arrest lines that accounted for up to half the jump length of the quenched specimen (Fig. 1d). The long crack jump time, approaching the crack arrest time, resulted in significant uncertainty in the measurements and scattering in the data (Table II). Thus crack propagation in the quenched samples almost lost the step-wise character.

Tests of specimens prepared from plaques slow-cooled overnight resulted in a fracture surface (Fig. 1c) more similar to the control. However, crack propagation was much faster than in the control. Both initiation and failure times as well as durations between jumps were shorter. These results are consistent with earlier observations that fatigue fracture is accelerated considerably if polyethylene samples are slow-cooled or annealed [17].

Very good correlation with the fatigue fracture behaviour of the control specimen was found in tests of specimens prepared from fast-cooled plaques (Fig. 1b). The fracture surfaces were almost indistinguishable in terms of the well-resolved striations and the fibrilated texture between arrest lines. Tests at other initial values of maximum stress intensity factor (1.0 and 1.3 $MPa\,m^{1/2}$) confirmed the good correlation (Tables I and II). Fig. 2 compares the kinetics of crack growth in specimens prepared from fast-cooled plaques with cumulative data on pipe specimens of both compact tension and arc-shaped geometry from a broad range of stress intensity factors. The pipe data are taken from a previous paper [19], and are presented in the form of a regression line on the Paris plot. The rate of

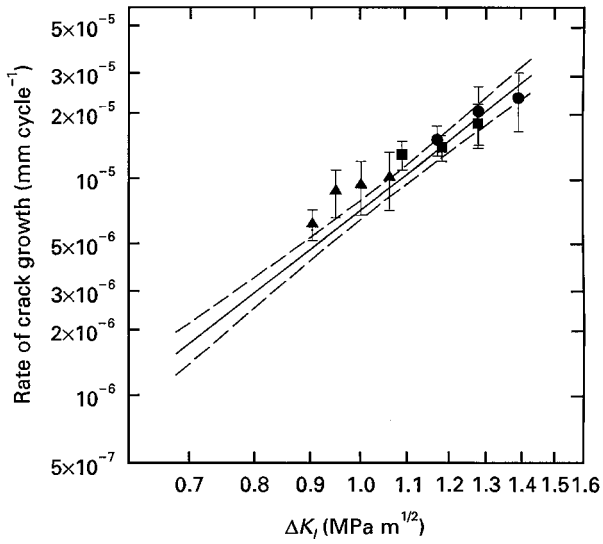

Figure 2 Fatigue crack propagation kinetics in compression-moulded compact tension specimens fast cooled at 30 °C/min^{-1} (●■▲) in comparison with the rate in specimens cut from pipe: (——) slope equal to 4.0, representing the regression of experimental data taken from [19]; (- - -) the 95% confidence level. $K_{I,max}$: (●) 1.3 $MPa\,m^{1/2}$, (■) 1.2 $MPa\,m^{1/2}$, (▲) 1.0 $MPa\,m^{1/2}$.

crack growth for discontinuous step-wise propagation was an average obtained by dividing the length of a jump by the duration. Because the value of stress intensity factor at the crack tip, K_I, increased as the crack propagated, every jump is presented on the Paris plot by a separate point. The value of K_I was determined for each crack tip position a by the standard expression $K_I(a)$ for a compact-tension specimen in accordance with ASTM D 5045-93. The change of stress intensity factor during a fatigue cycle ΔK_I, was calculated as

$$\Delta K_I = K_{I,max}(a)(1 - R) \quad (2)$$

where R, the minimum to maximum fatigue load ratio, was constant at $R = 0.1$.

The kinetic correlation presented in Fig. 2 and the fracture surface correspondence in Fig. 1a and b are good enough to justify the use of fast-cooling under pressure as the condition for compression-moulding thick polyethylene samples that will reproduce the fatigue crack resistance of real pipe. Although the

recommended procedure for compression-moulding specimens for the creep test is slow-cooling overnight [8,9], the data reported here for a wide range of crack growth rates lead to the conclusion that this practice is not appropriate for fatigue testing if the real pipe properties are to be simulated.

3.2. Ranking of polyethylene pipe resins

A blind study of four pipe resins (identified as A, B, C and D) was performed for the purpose of evaluating the fatigue test as a method for ranking candidate pipe resins. Using fast-cooling for specimen preparation, and fatigue testing conditions that produced step-wise crack propagation in the real pipe, the resins were first compared in terms of initiation and failure times (Table III). Testing was performed at two extreme values of stress intensity factor $K_{I,\max}$ equal to 1.0 and 1.3 MPa $m^{1/2}$. The fatigue resistance of the various resins differed considerably. In Table IV the fatigue data are compared with the failure time in the PENT creep test which was recently adopted as a standard for testing polyethylene pipe resins (ASTM F 1473-94). The ranking by fatigue initiation or failure time and PENT time is the same. However, fatigue testing times are much shorter than creep times.

The step-wise character of crack propagation in the resins under investigation is described in Table V, and fracture surfaces for tests at stress intensity factor $K_{I,\max} = 1.3$ MPa $m^{1/2}$ are compared in Fig. 3. In all cases, four crack jumps were well resolved by fractography and video observation. The discontinuous pattern of fracture in materials B and D at $K_{I,\max} = 1.0$ MPa $m^{1/2}$ represented six to seven jumps with the lengths being approximately half the length of those displayed in Fig. 3. However, only the initial three jumps were clearly distinguishable in materials A and C at $K_{I,\max} = 1.0$ MPa $m^{1/2}$, thereafter fracture proceeded in an almost continuous brittle manner. For each stress intensity factor, the jump lengths were nearly the same for all materials.

Kinetics of crack propagation in the materials tested is compared with the cumulative data for crack growth in pipe in Fig. 4 in the form of a Paris plot. The dependence of crack growth rate on the change of stress intensity factor in the fatigue cycle ΔK_I,

TABLE III Fatigue crack initiation and failure of different pipe resins

			$K_{I,\max} = 1.3$ MPa $(m)^{1/2}$		$K_{I,\max} = 1.0$ MPa $(m)^{1/2}$	
Material	Density (g/cm^3)	Crystallinity (Density)	Cycles to initiation (thousand)	Cycles to failure (thousand)	Cycles to initation (thousand)	Cycles to failure (thousand)
A	0.9328 ± 0.0002	58%	65 ± 5	213 ± 9	90 ± 7	570 ± 20
B	0.9410 ± 0.0002	63%	112 ± 7	268 ± 12	178 ± 15	940 ± 25
C	0.9518 ± 0.0003	70%	25 ± 3	79 ± 5	30 ± 3	210 ± 12
D	0.9526 ± 0.0001	71%	42 ± 5	137 ± 5	70 ± 5	270 ± 10
PIPE	0.9397 ± 0.0003	60%	65 ± 5	234 ± 20	82 ± 6	560 ± 30

TABLE IV Ranking of pipe resins by fatigue test ($K_{I,\max} = 1.3$ MPa $m^{1/2}$) and PENT

Material	Fatigue initiation time (hrs)	Fatigue failure time (hrs)	Fatigue Ranking	PENT time to failure (hrs)	PENT Ranking
A	19.0	57.5	2	850	2
B	31.0	74.5	1	2667	1
C	7.0	22.0	4	22	4
D	12.0	38.0	3	80	3

TABLE V Crack jump parameters for different pipe resins

$K_{I,\max}$ MPa $(m)^{\frac{1}{2}}$	Material	Length of jump 1 (mm)	Duration between jump 1 and 2 (thousand)	Length of jump 2 (mm)	Duration between jump 2 and 3 (thousand)	Length of jump 3 (mm)	Duration between jump 3 and 4 (thousand)
1.3	A	0.80 ± 0.10	50 ± 5	0.90 ± 0.10	40 ± 10	0.90 ± 0.15	25 ± 5
	B	0.72 ± 0.07	50 ± 5	0.83 ± 0.07	47 ± 5	0.90 ± 0.15	27 ± 10
	C	0.75 ± 0.05	17 ± 3	0.78 ± 0.07	15 ± 3	0.80 ± 0.07	9 ± 3
	D	0.70 ± 0.05	24 ± 3	0.70 ± 0.05	20 ± 3	0.76 ± 0.07	15 ± 3
	PIPE	0.80 ± 0.08	45 ± 6	0.80 ± 0.08	34 ± 10	0.85 ± 0.08	30 ± 10
1.0	A	0.45 ± 0.04	70 ± 7	0.45 ± 0.04	65 ± 10	—	—
	B	0.50 ± 0.04	122 ± 10	0.46 ± 0.04	108 ± 10	0.54 ± 0.04	92 ± 10
	C	0.42 ± 0.04	25 ± 4	0.38 ± 0.08	20 ± 7	—	—
	D	0.42 ± 0.04	44 ± 8	0.43 ± 0.08	36 ± 8	0.44 ± 0.08	35 ± 8
	PIPE	0.42 ± 0.06	68 ± 5	0.44 ± 0.06	50 ± 10	0.48 ± 0.06	50 ± 10

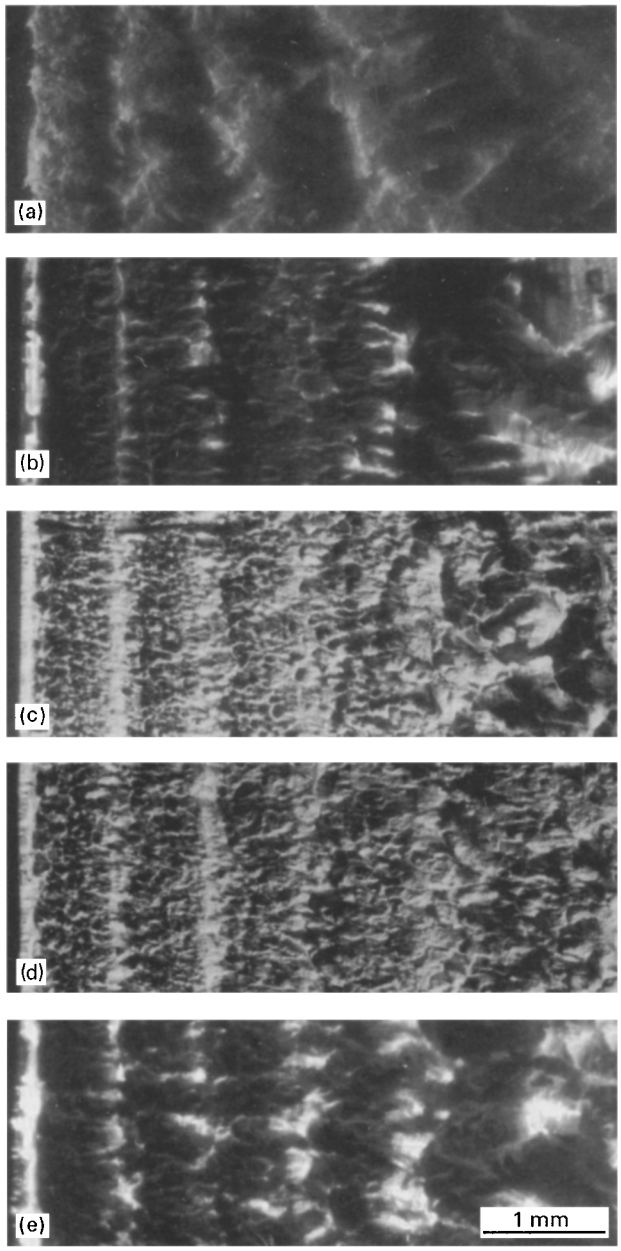

Figure 3 Fracture surfaces of pipe resins tested at an initial stress intensity factor of 1.3 MPa $m^{1/2}$: (a) A, (b) B, (c) C, (d) D, and (e) real pipe.

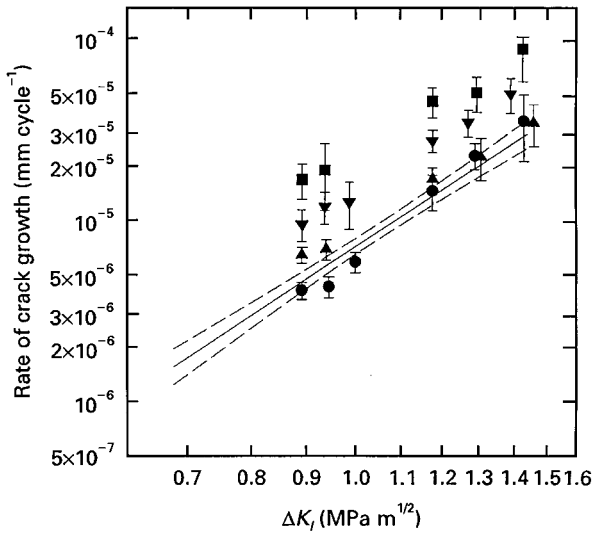

Figure 4 Fatigue crack propagation rate in four pipe resins (▲) A, (●) B, (■) C, (▼) D and (——, - - -) the rate in real pipe. The lines are described in Fig. 2.

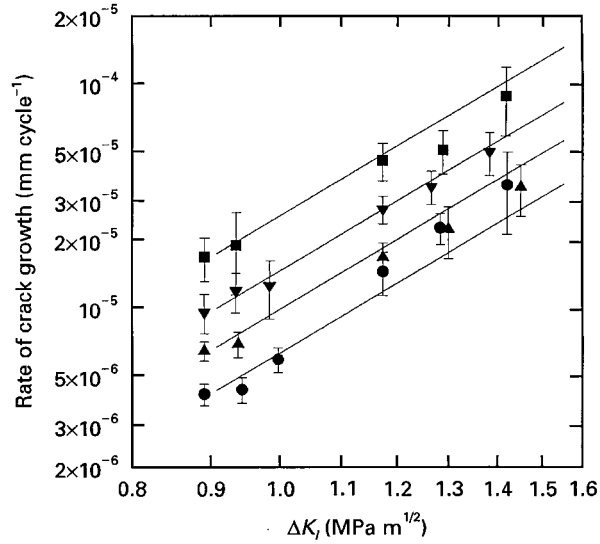

Figure 5 Fatigue crack propagation rate in four pipe resins (▲) A, (●) B, (■) C, (▼) D interpolated by straight lines of the slope equal to 4.0.

followed the same trend for all materials with a slope of about 4. Although tests at lower maximum stress intensity factor took more time, there was less experimental scatter. Ranking of the materials in terms of crack growth rate clearly followed the same order as obtained from initiation or failure time (Table III).

The fatigue crack resistance of pipe resins can be ranked by the traditional characteristics, initiation or failure time, as well as by the detailed kinetics of crack growth. All these fatigue parameters gave the same ranking order. However, the failure time encompasses processes of initiation, crack propagation and final ductile fracture, which have considerably different origins. Furthermore, initiation time for polyethylene pipe resins depends on notching procedure, and cannot be considered as a characteristic of the material only [23].

On the other hand, crack growth rate, w, relates to real material properties. For step-wise crack propagation, the crack growth rate is directly related to the size and lifetime of the damage zone ahead the crack tip. Although the rate changes as the crack grows because the stress intensity factor at the crack tip increases, this change can be predicted using the Paris relationship, $w \propto (\Delta K_I)^n$. The power n in this dependence is usually considered to vary with each material. However, the relevant data for different pipe resins [3, 10, 16, 24] are approximately covered by the range $n = 4.0 \pm 0.5$ that was defined as experimental scatter in determination of crack rate at discontinuous growth [19]. The use of $n = 4$ is justified by a simple theoretical model [25], and is also commonly accepted for calculating creep crack growth rate, w_c, in polyethylene pipes by a similar relationship $w_c \propto (K_I)^n$ [4, 26]. Therefore, this value can be assumed as approximately constant and equal to 4 for all pipe resins.

If so, only the initial crack growth rate, averaged over the first jump after initiation, is required to estimate the total kinetics of fracture. Tests at different initial values of ΔK_I can also be correlated in this way.

Fig. 5 shows how well the data for each resin tested can be described by a line with slope of 4. Each line originates at the point corresponding to the initial crack growth rate at $K_{I,\max} = 1.0$ MPa $m^{1/2}$. The deviation is of the order of the experimental error. This means that as long as the step-wise mechanism is observed, the ranking of polyethylene pipe resins is not affected by the magnitude of the stress intensity factor used in the test and hence by the fatigue load. Therefore, the initial crack growth rate measurement is sufficient for ranking, and a test can be terminated when rupture of the second membrane is complete. Measuring the duration between the first and second membrane ruptures, and the distance between respective arrest lines on the fracture surface, provides a straightforward way to obtain this information. The test time is significantly shortened in this way, and therefore the lower value of ΔK_I can be used to get rapid and accurate results.

4. Conclusion

A fatigue test of standard compact-tension specimens performed (a) at loading conditions that simulate the step-wise fracture mechanism in real pipe, and (b) with compression-moulded samples that reproduce the fatigue properties of real pipe, differentiated crack resistance of polyethylene pipe resins and ranked them in the same order as a creep test. Kinetics of the first jump after initiation furnished sufficient information to evaluate crack resistance and rank materials. Tensile–tensile fatigue tests with maximum stress intensity factor equal to 1.0 MPa $m^{1/2}$ and minimum-to-maximum fatigue load ratio of 0.1 were best for revealing differences among polyethylene pipe resins.

Acknowledgements

The research was generously funded by the Gas Research Institute (contract number 5090-260-2031). The financial assistance of BP Chemicals Ltd is also gratefully acknowledged.

References

1. N. BROWN, X. LU, Y.-L. HUANG and R. QIAN, *Macromol. Chem.* **41** (1995) 55.
2. J. J. STREBEL and A. MOET, *J. Mater. Sci.* **27** (1992) 2981.
3. H. NISHIMURA, A. NAKASHIBA, M. NAKAKURA and K. SASAI, *Polym. Eng. Sci.* **33** (1993) 895.
4. M. F. KANNINEN, P. E. O'DONOGHUE, C. H. POPELAR and V. H. KENNER, *Eng. Fract. Mech.* **36** (1990) 903.
5. Y. ZHOU, X. LU and N. BROWN, *Polym. Eng. Sci.* **31** (1991) 711.
6. M. B. BARKER, J. BOWMAN and M. BEVIS, *J. Mater. Sci.* **18** (1983) 1095.
7. K. SEHANOBISH, A. MOET, A. CHUDNOVSKY and P. P. PETRO, *J. Mater. Sci. Lett.* **4** (1985) 890.
8. X. LU, R. QIAN and N. BROWN, *J. Mater. Sci.* **26** (1991) 917.
9. N. BROWN and X. LU, in "Proceedings of 12th Plastic Fuel Gas Pipe Symposium", Boston, MA, September 1991, p. 128.
10. Y. ZHOU and N. BROWN, *Polym. Eng. Sci.* **33** (1993) 1421.
11. P. T. REYNOLDS and C. C. LAWRENCE, *J. Mater. Sci.* **28** (1993) 2277.
12. E. SHOWAIB and A. MOET, *ibid.* **28** (1993) 3617.
13. X. LU, A. McGHIE and N. BROWN, *J. Polym. Sci. B Polym. Phys.* **30** (1992) 1207.
14. M. KLEIN, N. BROWN and A. MOET, in "SPE Conference Proceedings/ANTEC'90", Dallas, TX, May 1990, p. 1487.
15. N. BROWN, M. KLEIN, A. MOET and H. NISHIMURA, in "Proceedings of 12th Plastic Fuel Gas Pipe Symposium", Boston, MA, September 1991, p. 2.
16. T. L. CARTE, M. KLEIN and A. MOET, In "SPE Conference Proceedings/ANTEC'94", San Francisco, CA, May 1994, Part 3, p. 3228.
17. J. RUNT and M. JACQ, *J. Mater. Sci.* **24** (1989) 1421.
18. J. J. STREBEL and A. MOET, *Int. J. Fract.* **54** (1992) 21.
19. A. SHAH, E. V. STEPANOV, A. HILTNER, E. BAER and M. KLEIN, *Int. J. Fract.* **84** (1997) 159.
20. B. WUNDERLICH, "Macromolecular Physics", Vol. 2 (Academic Press, New York, 1976).
21. IU. K. GODOVSKY, "Thermophysical properties of polymers" (Springer, Berlin, 1992).
22. H. C. CARSLAW and J. C. JAEGER, "Conduction of heat in solids" (Clarendon Press, Oxford, 1986).
23. X. LU, R. QIAN and N. BROWN, *J. Mater. Sci.* **26** (1991) 881.
24. Y.-Q. ZHOU and N. BROWN, *ibid.* **24** (1989) 1458.
25. A. CHUDNOVSKY and A. MOET, *Polym. Eng. Sci.* **22** (1982) 922.
26. N. BROWN and X. LU, *Int. J. Fract.* **69** (1995) 371.

Received 16 April 1997
and accepted 22 April 1998